N-VINYLPYRROLIDONE – BASED INTERPENETRATING POLYMERIC NETWORKS INCORPORATING FUNCTIONALIZED CARBON NANOFIBERS

Alice-Ionela PODARU[1], Andreea Elena MOLDOVAN[2,*], Mariana IONITA[3,4], Edina RUSEN[5], Aurel DIACON[6], Gabriela TOADER[7], Raluca Elena GINGHINA[8], Ana-Mihaela GAVRILA[9]

Interpenetrating polymeric networks containing poly(N-vinyl-2-pyrrolidone-co-2-acrylamido-2-methyl-1-propane sulfonic acid) and polyvinyl alcohol reinforced with different concentrations of pristine carbon nanofibers (CNFs) or poly(ethylene glycol) – functionalized carbon nanofibers were prepared by photopolymerization. The synthesized hydrogels were characterized by Fourier-transform infrared spectroscopy (FT-IR), scanning electron microscopy (SEM), thermogravimetric analysis (TGA), swelling investigations, mechanical tests to evaluate the influence of the CNFs and their functionalization on the properties of the hydrogels.

Keywords: carbon nanofibers, interpenetrating polymeric networks, N-vinyl-2-pyrrolidone, nanocomposite films

1. Introduction

Interpenetrating polymeric networks (IPNs) are new-generation materials that can be used for a broad range of applications. The term interpenetrating polymer network (IPN) refers to a material composed of two or more networks that are partially interconnected on a molecular level without a covalent bond between them [1]. Still, they cannot be disconnected without breaking chemical bonds since

[1] PhD student, Faculty of Chemical Engineering and Biotechnologies, University POLITEHNICA of Bucharest, and Military Technical Academy „FERDINAND I", Bucharest, Romania, e-mail: alice.podaru@mta.ro;
[2] Lect., PhD, Military Technical Academy „FERDINAND I", Bucharest, Romania, e-mail: andreea.moldovan@mta.ro; corresponding author;
[3] Prof., Advanced Polymer Materials Group, Dept. of Bioresources and Polymer Science, and Faculty of Medical Engineering, University POLITEHNICA of Bucharest, Romania, e-mail: mariana.ionita@polimi.it;
[4] Prof.. eBio-Hub Research Centre, University Politehnica of Bucharest-Campus, Iuliu Maniu 6, 061344, Bucharest, Romania, e-mail: mariana.ionita@polimi.it;
[5] Researcher II, PhD, Faculty of Chemical Engineering and Biotechnologies, University POLITEHNICA of Bucharest, Romania, e-mail: edina_rusen@yahoo.com;
[6] Assoc. prof., PhD, Military Technical Academy „FERDINAND I", Bucharest, Romania, e-mail: aurel_diacon@yahoo.com;
[7] Assoc. prof., PhD, Military Technical Academy „FERDINAND I", Bucharest, Romania, e-mail: gabriela.toader@mta.ro;
[8] Researcher III, PhD, Research and Innovation Center for CBRN Defense and Ecology, Bucharest, Romania, e-mail: raluca.ginghina@nbce.ro;
[9] Researcher II, PhD, National Institute for Research & Development in Chemistry and Petrochemistry ICECHIM, Bucharest, Romania, e-mail: anamihaela.florea@gmail.com.

they are interlaced [1]. IPNs offer many advantages compared to single-network crosslinked polymers, including broadly tunable physical characteristics, thermal stability, and chemical resistance [2-4]. The reinforcement of IPN with distinct nanofillers has been shown to provide additional strength [5, 6]. Wang et al. [7] reported "super-tough double networks (DNs)" reinforced with nanofiller with remarkable mechanical resistance. Nanoscale fillers have the significant advantage that a small quantity of filler is sufficient to cause substantial improvement of necessary properties due to the high surface to volume ratio of the nanoparticles. However, the obtaining of a good/uniform distribution of nanofillers is critical [8]. Conversely, the nanoparticles dispersion can be enhanced by further functionalization of their surfaces which can allow covalent bonds to be formed with the polymer template. Numerous benefits from the simultaneous incorporation of nanofiller and IPNs in a one-step synthesis were reported in the literature [9-11].

Significant attention has been given to the water interaction characteristics of the IPNs, specifically water intake or the adsorbed water effects on the properties of the polymeric network [8], for applications related to the biomedical field, wound dressing, tissue engineering, etc. For instance, the use of a monomer like2-acrylamido-2-methyl-1-propane sulfonic acid (AMPSA) may guarantee high water absorption. The AMPSA-based hydrogels usually reach high hydration levels because the sulfonic acid functional groups in AMPSA are extremely hydrophilic [12]. Moreover, due to its structural resemblance to glycosaminoglycan (a component of the extracellular matrix and a key player in wound healing), the literature has described AMPSA as a presumably biomimetic monomer [13]. N-Vinylpyrrolidone (NVP) - based polymers are also well-recognized for their biocompatibility[14]. Because of the exceptional wettability of poly(N-vinyl-2-pyrrolidone), NVP has recently been used as one of the components in the manufacture of contact lenses [14]. Polyvinyl alcohol (PVA) is a hydrophilic polymer widely used for its excellent film-forming properties and exceptional mechanical strength. Due to their biocompatibility and biodegradability, PVA-based IPN hydrogels are commonly used in biomedical applications, medical devices, etc. [15, 16]. Poly(ethylene glycol) is another widely-used polymer in the biomedical field since it is harmless, biodegradable, biocompatible, and nonantigenic to human tissues [13]. Carbon allotropes, such as carbon nanotubes (CNTs) or carbon nanofibers (CNFs) have been investigated and successfully utilized as reinforcing agents for IPNs in several biomedical applications, including biosensors [17], drug delivery [18], scaffolds [19], etc.

Numerous scientists have investigated the characteristics of PVA-NVP-based materials: Lu et al. [20] reported poly(vinyl alcohol)/poly(vinyl pyrrolidone) - based IPN membranes; Kim et al. [21] described the construction of interpenetrating polymer network (IPN) hydrogels employing poly(vinyl alcohol) and 1-vinyl-2-pyrrolidone networks obtained by photopolymerization using 2,2-

dimethoxy-2-phenylacetophenone as a photoinitiator and N,N-methylenebisacrylamide as a crosslinker. Yet, few studies have approached PVA-NVP-AMPSA ternary blends for composite IPNs, and even fewer studies have utilized carbon nanofibers in these sorts of IPNs.

This study aimed to examine the effect of CNFs and their functionalization on the mechanical and physical properties of IPNs comprising poly(N-vinyl-2-pyrrolidone-co-2-acrylamido-2-methyl-1-propane sulfonic acid) and polyvinyl alcohol. IPN matrices were reinforced with various concentrations of pristine CNF or polyethylene glycol-functionalized CNFs. This research required the development and characterization of novel PVA-NVP-AMPSA-CNF-PEG formulations that afforded innovative IPNs with remarkable mechanical properties. To the best of our knowledge, no such material has been found to date in the literature. The improved mechanical characteristics of herein reported nanocomposites, combined with their high hydrophilicity, justifies their possible application in different areas such as biomedical devices, decontamination materials, etc.

2. Materials and Methods

a. Materials

Carbon nanofibers (**CNF**, carbon nanofibers graphitized, platelets (conical), >98% carbon basis, D × L - 100 nm × 20-200 μm, Sigma Aldrich), thionyl chloride (**$SOCl_2$**, ReagentPlus®, ≥99%, Sigma Aldrich), sulfuric acid (**H_2SO_4**, ACS reagent, 95.0-98.0%, Sigma Aldrich), nitric acid (**HNO_3**, ACS reagent, 70%, Sigma Aldrich), Poly(ethylene glycol) (**PEG400**, average M_n 400 Da, Sigma Aldrich), Poly(vinyl alcohol) (**PVA**, average Mw 85,000-124,000, 87-89% hydrolyzed, Sigma Aldrich), 2-Acrylamido-2-methyl-1-propanesulfonic acid (**AMPSA**, 99%, Sigma Aldrich), N,N′-methylenebisacrylamide (**MBA**, 99%, Sigma Aldrich), tetrahydrofuran (**THF**, ≥99.9%, Sigma Aldrich), 2-hydroxy-4′-(2-hydroxyethoxy)-2-methylpropiophenone (**Ph-In**, 98%, Sigma-Aldrich), were used as received. 1-Vinyl-2-pyrrolidone (**NVP**, sodium hydroxide as an inhibitor, ≥99%, Sigma Aldrich) was distilled and stored at 4°C before the synthesis steps.

b. Methods

if. Functionalization of CNF

The CNFs were functionalized in three steps, similar to the ones described in ref. [22] for MWCNTs. Briefly, 1 g of pristine CNFs were dispersed in a 50 mL mixture of H_2SO_4 (98%) / HNO_3 (68%) 3:1 (v/v) via sonication for 12 h. The mixture was further diluted with water, followed by filtration on a PTFE membrane, and washed several times with deionized water. The resulting CNF-COOH were dried overnight in a vacuum oven at 80°C. The next step consisted of the reaction between CNF-COOH and thionyl chloride ($SOCl_2$) to form acyl chlorides on the

surface of the CNFs. For this step, CNF-COOH were dispersed in $SOCl_2$ and maintained under magnetic stirring at 65°C for 24 h. After that, the dispersion was repeatedly washed with THF, filtered on a PTFE membrane, and dried overnight at 30°C.The last step consisted of attaching the PEG400 chains to the surface of the acyl chloride-functionalized CNFs. For this purpose, the dried acyl chloride-functionalized CNFs were dispersed in PEG400 and maintained under continuous stirring for 48 h at 120°C. The resultant dispersion containing the CNFs functionalized with poly(ethylene glycol) chains (CNF-PEG400) was washed with THF and filtered on a PTFE membrane, followed by drying at 40°C for 48 h. The above-described steps are illustrated in **Fig. 1**.

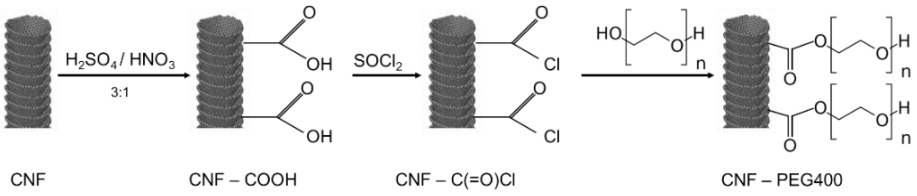

Fig. 1. CNF functionalization steps

ii. Synthesis of nanocomposite IPNs films

The IPN films were obtained through photopolymerization using a UV lamp (low-pressure Hg UV lamp, λ_{em} = 254 nm), in rectangular (silicone rubber-sealed) glass molds (12 × 12 × 0.2 cm). For the blank sample (**Bk**), the monomers (3.33g **NPV** and 1.35g **AMPSA**), the crosslinker (0.1g **MBA**), and the photoinitiator (0.018g **Ph-In**) were dissolved in freshly prepared 5g of **PVA** aqueous solution (5wt.%). For the nanocomposite IPN formulations (**0.05% CNF, 0.1% CNF, 0.2% CNF, 0.05% CNF-PEG400, 0.1% CNF-PEG400, 0.2% CNF-PEG400**), the appropriate amounts of CNFs/CNF – PEG400 (according to ***Table 1***) were firstly dispersed via ultrasonication in the freshly prepared 5g of **PVA** aqueous solution (5 wt.%), subsequently continued by the addition of the monomers (3.33g **NPV** and 1.35g **AMPSA**), the crosslinker (0.1g **MBA**), and the photoinitiator (0.018g **Ph-In**). The complete curing of the IPN films was observed after approximately 40 minutes of UV exposure. Sample codes of the IPN films obtained are detailed in **Table 1**.

Table 1

IPNs nanofiller composition

Sample code	CNF, wt.%	CNF - PEG400, wt.%
Bk	-	-
0.05% CNF	0.05	-
0.1% CNF	0.10	-
0.2% CNF	0.20	-
0.05% CNF-PEG400	-	0.05
0.1% CNF-PEG400	-	0.10
0.2% CNF-PEG400	-	0.20

c. Characterizations

SEM analysis CNF-PEG400 was performed using a ZEISS Sigma© 500 VP instrument at 1 keV, InlensSE detector, magnifications up to 100k. SEM imaging of the lyophilized nanocomposite films was executed on a Hitachi TM4000plus II instrument, 15kV. Before SEM investigations, the samples were gold-sputtered (a thin layer ~5nm) with a Sputter Coater Q150R ES Plus (Quorum). The thermal properties of the materials were assessed on a Netzsch TG 209 F3 Tarsus equipment, with a 10°C/min heating rate, temperature range: 25°C− 900°C, 20 mL/min nitrogen flow rate, on samples weighting 4 mg, in an alumina (Al_2O_3) crucible. FT-IR analysis was performed on a Spectrum Two FTIR spectrometer (PerkinElmer)with a MIRacleTM Single Reflection ATR-PIKE Technologies at 4 cm^{-1} resolution, summing 32 scans in the 4000−600 cm^{-1} region. The swelling ability of the composite IPNs was estimated according to refs.[23-25]. Thus, the swelling degree of IPNs was determined using the gravimetric technique, which involved immersing samples in DI water until they reached a constant weight at 37 °C. These swelling investigations were performed in duplicate, and the mean values for each sample were reported. Uniaxial compressive tests were performed at 2mm/min, utilizing compression clamps (Ø40mm) on a DMA 850 from TA Instruments. Five fully swollen disc specimens from each sample were subjected to compression on a stress ramp, and mean values were reported. The DMA 850 instrument was also used in "shear-sandwich" clamping mode to measure the frequency-dependent shear modulus, at a constant strain of 1%, on a logarithmic increase of frequency from 0.1 to 10Hz.

3. Results

The first analytical investigations aimed to characterize the functionalized carbon nanofibers (CNF-PEG400). SEM images in Fig. 2 revealed the existence of PEG on the surface of the CNFs. Moreover, it can be observed that the functionalization procedure did not alter the overall morphology of the CNFs. However, it seems that some CNFs were shortened, probably due to the H_2SO_4/HNO_3 treatment combined with prolonged ultrasonication.

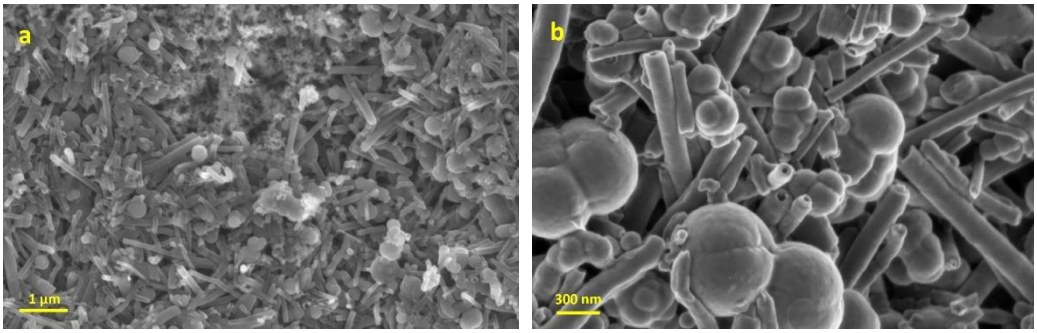

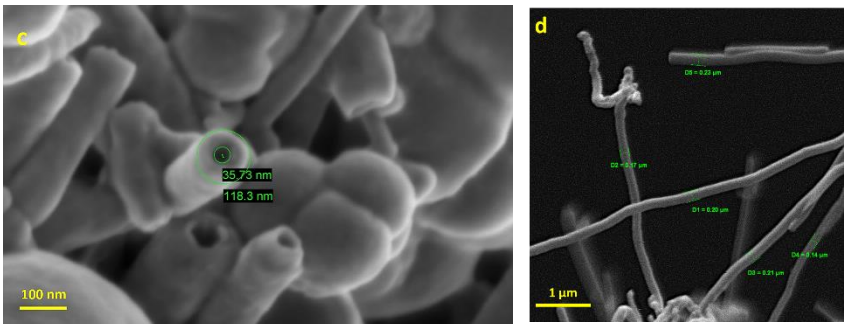

Fig. 2. SEM images of CNF-PEG400 at different magnifications (a-c); pristine CNFs (d)

TGA analysis offered information on the thermal stability and degree of functionalization of the PEG400 modified CNFs compared to the pristine CNFs. The results obtained are comparatively illustrated in Fig. 3. The weight loss steps visible on the TGA and DTG plots of CNF-PEG400 sample are caused by the adsorbed water release (3% corresponding to the temperature range 25-150°C) and by the decomposition of the PEG chains (with T_{max} 328°C) which accounts for approximatively 22% [26]. In contrast, pristine CNFs displayed good thermal stability until 550-600°C.

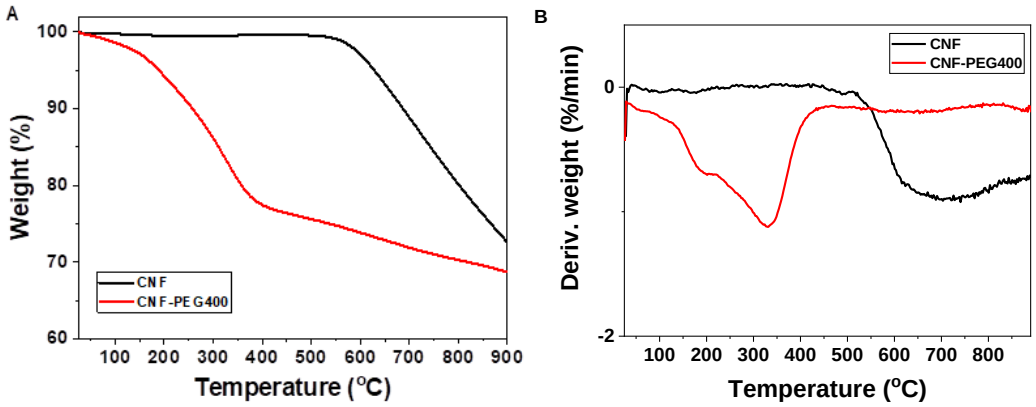

Fig. 3. TGA (A) and DTG (B) analyses of non-functionalized CNFs and CNF-PEG400

The subsequent step in this study consisted of employing various concentrations of pristine CNF or CNF-PEG400 as nanofillers for obtaining a series of composite IPNs, by employing the afore mentioned procedure to evaluate their properties, and to compare their reinforcing abilities.

The chemical composition of the synthesized materials was investigated using FT-IR analysis. FT-IR spectrum of CNF-PEG400 (Fig. 4.a) comprises the C=O stretching characteristic peak at 1706 cm^{-1}. Analogous adsorption bands were visible in the FT-IR spectra for all IPNs synthesized in this study; consequently, the FT-IR spectrum of Bk was selected for display (Fig. 4.b). The two broad overlapping peaks from 3400 and 3315 cm^{-1}could be assigned to ν_{N-H} and ν_{O-H}

stretching vibrations, respectively. The hydrophilic amide carbonyl group N–C=O from NVP is visible at 1645cm^{-1}. At 1040 cm^{-1}, the C-N stretching vibration ($\nu_{C\text{-}N}$) is detectable. S=O stretching from AMPSA can be attributed to the absorption bands around 1387 cm^{-1}.

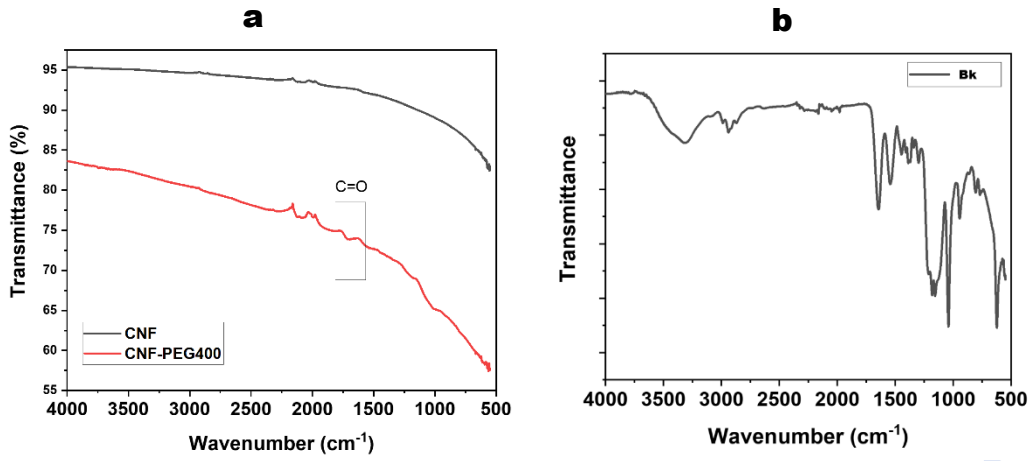

Fig. 4. FT-IR spectra: (a) CNF and CNF-PEG400; (b) Bk sample

The photograph of IPNs (in equilibrium swollen state) from Fig. 5.a reveals a clear difference between the quality of dispersion of CNF vs. CNF-PEG400. As expected, the functionalization of the CNFs with PEG400 ensured a much more homogenous distribution of the nanofiller inside the polymeric matrix. The first parameter investigated for the nanocomposite IPNs was the degree of swelling in water. The swelling degree is mainly influenced by: crosslinking density, nanofiller concentration, and polymer-solvent interaction[27].

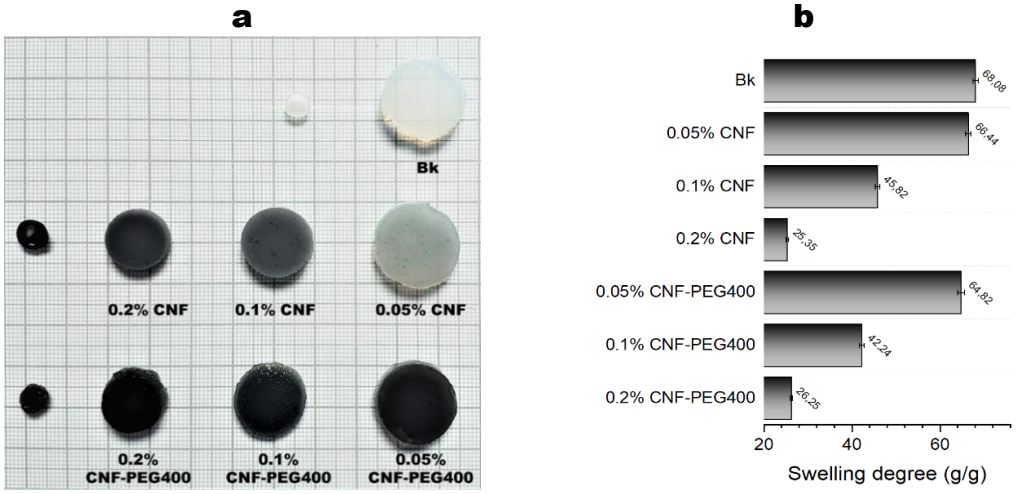

Fig. 5. (a) Xerogels and equilibrated-swollen state IPNs; (b) Equilibrium swelling degree of IPNs

From Fig. 5.b, it can be observed that the swelling degree was noticeably influenced by the nanofiller concentration. Consequently, the swelling degree decreased with the increase of CNF concentration.

The morphology of the resulting composite IPNs can be visualized in Fig. 6. Thus, the SEM images of the lyophilized IPNs revealed distinct morphologies depending on the nanofiller content. As shown in Fig. 6, the pores have a much more regular, homogeneous geometry as the nanofiller concentration increases. The samples containing pristine CNF displayed a distinct morphology due to the less effective dispersion in the polymeric matrix, which might have caused CNF aggregation in some areas.

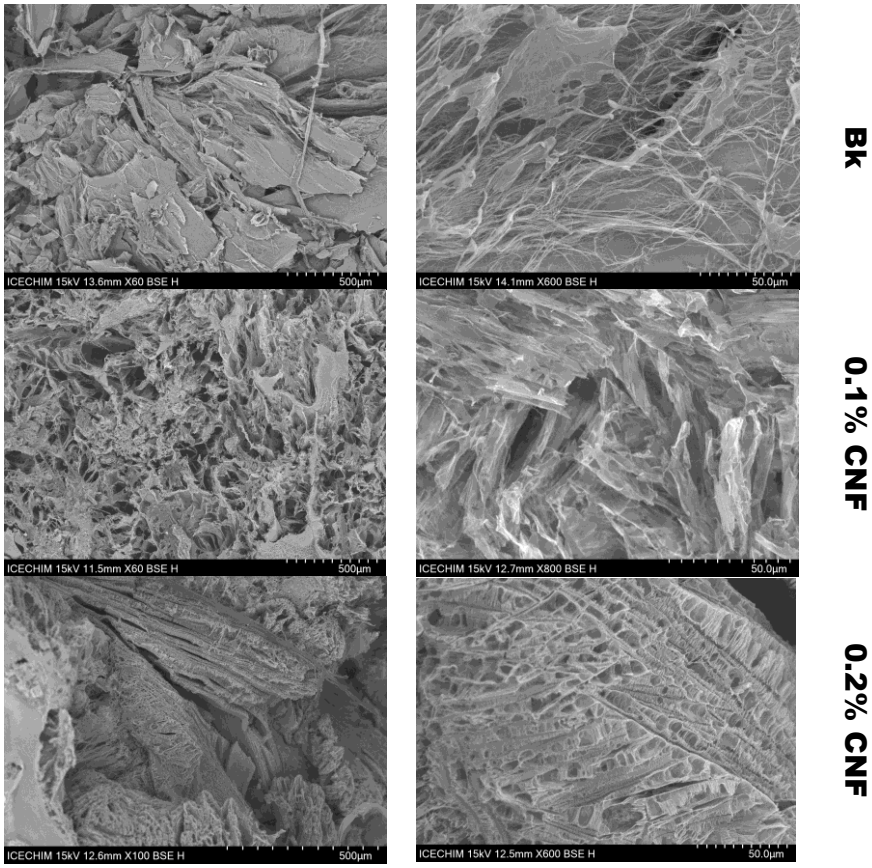

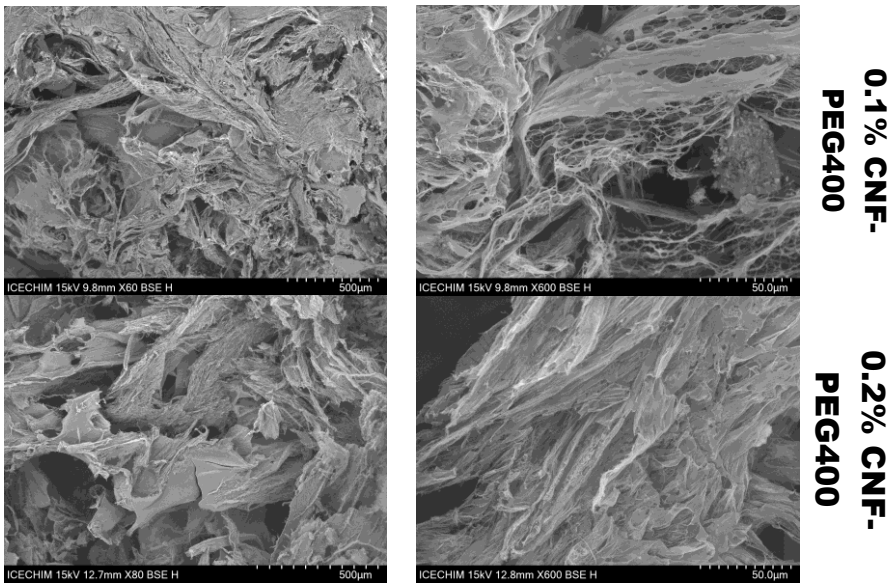

Fig. 6. SEM images of the lyophilized IPNs

Fig. 7 illustrates the results obtained for uniaxial compressive and frequency-dependent shear tests. Shear measurements facilitated the interpretation of the viscoelastic nature of the synthesized IPNs, as well as the effect of the nanofiller on their strength when subjected to shear forces. The storage modulus plots (Fig.7.a) indicate that the higher values of G', brought by the presence of the CNF-PEG400 in the polymeric matrix, suggest that these nanofillers induced a higher strengthening effect of the IPNs than pristine CNFs.

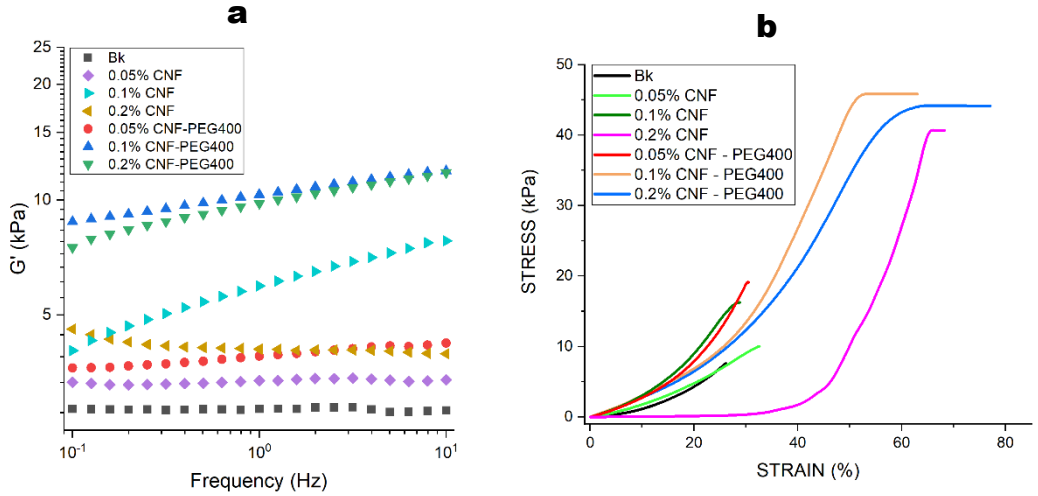

Fig. 7. (a) Storage modulus vs. frequency; (b) Compressive stress-strain curves

Moreover, at concentrations of nanofiller higher than 0.1%, it has been observed that this stiffening effect is slightly reduced, probably due to the less homogenous dispersion inside the IPNs at higher CNF or CNF-PEG concentrations. The same trends can be observed from the compressive stress-strain curves (Fig.7.b). Thus, the introduction of pristine CNFs led to a slight improvement in mechanical resistance. Still, this mechanical resistance should also be correlated with their lower water uptake capacity. Finally, the positive influence of CNF-PEG nanofiller in terms of the mechanical resistance of the resulting IPNs is much more noticeable. Thus, this investigation confirmed that the functionalization of the CNFs with PEG400 ensured an improved dispersion of the nanofiller within the IPN. Consequently, the homogenous dispersion of the nanofiller induced higher mechanical resistance to compressive loading. However, it seems that at CNF-PEG400 concentrations higher than 0.1 wt.%, the toughness of the equilibrium-swelled IPNs slightly decreased, probably because of their less efficient dispersion in the polymeric matrix.

6. Conclusions

This research started with the functionalization of the CNFs with PEG400. TGA and SEM analyses confirmed the chemical attachment of PEG chains on the surface of the carbon nanofibers. Further, this paper describes the synthesis and characterization of seven distinct types of IPNs: three containing different concentrations of pristine CNF, the other three different concentrations of CNF-PEG, and one blank sample. All six composite samples comprised the same polymeric matrix configuration as the blank sample, based on poly (N-vinyl-2-pyrrolidone-co-2-acrylamido-2-methyl-1-propane sulfonic acid) and polyvinyl alcohol. The investigations demonstrated the positive effect of CNFs on the mechanical and physical properties of IPNs. In this case, remarkably higher mechanical resistance, a 5-fold stress resistance increase compared to the blank formulation, was achieved at a 0.1 % (weight %) CNF-PEG400 content. Finally, the improved mechanical properties of herein-reported novel IPNs formulations (PVA-NVP-AMPSA-CNF-PEG) and their high hydrophilicity recommend them for various biomedical technologies, water treatment, etc.

Acknowledgments

This work was financially granted by the Ministry of Research, Innovation, and Digitalization (UEFISCDI) through ctr. no. PD 69/2022 and ctr. no. 672 PED/2022. Alice Podaru gratefully acknowledges the financial support from the European Social Fund from the Sectoral Operational Programme Human Capital 2014-2020, through the Financial Agreement with the title "Training of Ph.D. students and postdoctoral researchers to acquire applied research skills -SMART", Contract no. 13530/16.06.2022 - SMIS code: 153734. Ana-Mihaela Gavrila also

acknowledge the opportunity given by the Ministry of Research, Innovation and Digitalization (Romanian Funding Agency UEFISCDI), through the supporting project no. 604PED/2022.

R E F E R E N C E S

[1] *M.K. Purkait, M.K. Sinha, P. Mondal, R. Singh*. Stimuli responsive polymeric membranes: smart polymeric membranes: Academic Press; 2018.

[2] *E.S. Dragan*. Advances in interpenetrating polymer network hydrogels and their applications. **86**, (11), 2014, 1707-1721.

[3] *U. Farooq, J. Teuwen, C. Dransfeld*. Toughening of Epoxy Systems with Interpenetrating Polymer Network (IPN): A Review. Primary Toughening of Epoxy Systems with Interpenetrating Polymer Network (IPN): A Review2020.

[4] *W. Xiao, J. He, J.W. Nichol, L. Wang, C.B. Hutson, B. Wang, et al.* Synthesis and characterization of photocrosslinkable gelatin and silk fibroin interpenetrating polymer network hydrogels. Acta Biomaterialia, **7**, (6), 2011, 2384-2393.

[5] *K.L. Moffat, K. Goon, F.T. Moutos, B.T. Estes, S.J. Oswald, X. Zhao, et al.* Composite Cellularized Structures Created from an Interpenetrating Polymer Network Hydrogel Reinforced by a 3D Woven Scaffold. Macromolecular Bioscience, **18**, (10), 2018, 1800140.

[6] *S. Chaturvedi, P.N. Dave*. Chapter 7 - Role of Nanofillers in Blends, Interpenetrating Polymer Networks, and Gels of Unsaturated Polyester Resin Polymers. In: Thomas S., Hosur M., Chirayil C. J., editors. Unsaturated Polyester Resins: Elsevier; 2019. p. 173-180.

[7] *Q. Wang, R. Hou, Y. Cheng, J. Fu*. Super-tough double-network hydrogels reinforced by covalently compositing with silica-nanoparticles. Soft Matter, **8**, (22), 2012, 6048-6056.

[8] *P. Klonos, V. Chatzidogiannaki, K. Roumpos, E. Spyratou, P. Georgiopoulos, E. Kontou, et al.* Structure–properties investigations in hydrophilic nanocomposites based on polyurethane/poly(2–hydroxyethyl methacrylate) semi-interpenetrating polymer networks and nanofiller densil for biomedical application. Journal of Applied Polymer Science, **133**, (11), 2016.

[9] *J. Djonlagić, D. Žugić, Z. Petrović*. High strength thermoresponsive semi-IPN hydrogels reinforced with nanoclays. Journal of Applied Polymer Science, **124**, (4), 2012, 3024-3036.

[10] *C.W. Peak, J.J. Wilker, G. Schmidt*. A review on tough and sticky hydrogels. Colloid and Polymer Science, **291**, 2013, 2031-2047.

[11] *M. Kheirabadi, R. Bagheri, K. Kabiri*. Swelling and mechanical behavior of nanoclay reinforced hydrogel: single network vs. full interpenetrating polymer network. Polymer Bulletin, **72**, (7), 2015, 1663-1681.

[12] *M. Manohar, D. Kim*. Synergistic Effect of 2-Acrylamido-2-methyl-1-propanesulfonic Acid on the Enhanced Conductivity for Fuel Cell at Low Temperature. Membranes, **10**, (12), 2020, 426.

[13] *A. Kapanya, R. Somsunan, W. Phasayavan, R. Molloy, S. Jiranusornkul*. Effect of molecular weight of poly(ethylene glycol) as humectant in interpenetrating polymer network hydrogels based on poly(sodium AMPS) and gelatin for wound dressing applications. International Journal of Polymeric Materials and Polymeric Biomaterials, **70**, (7), 2021, 496-506.

[14] *D. Singh, V. Choudhary, V. Koul*. Radiation synthesis of interpenetrating polymer networks based on N-vinyl pyrrolidone – acrylic acid copolymer and gelatin. I. Swelling, morphology, and thermal characterization for biomedical applications. Journal of Applied Polymer Science, **104**, (3), 2007, 1456-1463.

[15] *Y. Lu, D. Wang, T. Li, X. Zhao, Y. Cao, H. Yang, et al.* Poly(vinyl alcohol)/poly(acrylic acid) hydrogel coatings for improving electrode–neural tissue interface. Biomaterials, **30**, (25), 2009, 4143-4151.
[16] *Y.J. Kim, J. Min*. Property modulation of the alginate-based hydrogel via semi-interpenetrating polymer network (semi-IPN) with poly(vinyl alcohol). International Journal of Biological Macromolecules, **193**, 2021, 1068-1077.
[17] *P. Hu, J. Zhang, Z. Wen, C. Zhang*. Network single-walled carbon nanotube biosensors for fast and highly sensitive detection of proteins. Nanotechnology, **22**, (33), 2011, 335502.
[18] *P.D. Boyer, H. Shams, S.L. Baker, M.R. Mofrad, M.F. Islam, K.N. Dahl*. Enhanced intracellular delivery of small molecules and drugs via non-covalent ternary dispersions of single-wall carbon nanotubes. Journal of Materials Chemistry B, **4**, (7), 2016, 1324-1330.
[19] *B. Gorain, H. Choudhury, M. Pandey, P. Kesharwani, M.M. Abeer, R.K. Tekade, et al.* Carbon nanotube scaffolds as emerging nanoplatform for myocardial tissue regeneration: A review of recent developments and therapeutic implications. Biomedicine & Pharmacotherapy, **104**, 2018, 496-508.
[20] *J. Lu, Q. Nguyen, J. Zhou, Z.-H. Ping*. Poly(vinyl alcohol)/poly(vinyl pyrrolidone) interpenetrating polymer network: Synthesis and pervaporation properties. Journal of Applied Polymer Science, **89**, (10), 2003, 2808-2814.
[21] *S.J. Kim, S.J. Park, K.H. An, N.G. Kim, S.I. Kim*. Water behavior of poly(vinyl alcohol)/poly(vinylpyrrolidone) interpenetrating polymer network hydrogels. Journal of Applied Polymer Science, **89**, (1), 2003, 24-27.
[22] *S. Sharmeen, A.F.M.M. Rahman, M.M. Lubna, K.S. Salem, R. Islam, M.A. Khan*. Polyethylene glycol functionalized carbon nanotubes/gelatin-chitosan nanocomposite: An approach for significant drug release. Bioactive Materials, **3**, (3), 2018, 236-244.
[23] *J. Macron, B. Bresson, Y. Tran, D. Hourdet, C. Creton*. Equilibrium and out-of-equilibrium adherence of hydrogels against polymer brushes. Macromolecules, **51**, (19), 2018, 7556-7566.
[24] *C.M. Ninciuleanu, R. Ianchiş, E. Alexandrescu, C.I. Mihăescu, C. Scomoroşcenco, C.L. Nistor, et al.* The effects of monomer, crosslinking agent, and filler concentrations on the viscoelastic and swelling properties of poly (methacrylic acid) hydrogels: A comparison. Materials, **14**, (9), 2021, 2305.
[25] *G. Toader, R.E. Ginghina, A. Diacon, E. Rusen, A.E. Bratu, A. Podaru, et al.* Design and Application of Photocrosslinkable Hydrogel Films for Fast and Efficient Decontamination of Chemical Warfare Agents. ACS Applied Polymer Materials, **5**, (1), 2023, 877-891.
[26] *M.A. Salam, R. Burk*. Synthesis and characterization of multi-walled carbon nanotubes modified with octadecylamine and polyethylene glycol. Arabian Journal of Chemistry, **10**, 2017, S921-S927.
[27] *S. Khan, N.M. Ranjha*. Effect of degree of cross-linking on swelling and on drug release of low viscous chitosan/poly(vinyl alcohol) hydrogels. Polymer Bulletin, **71**, (8), 2014, 2133-2158.